Carla Proença,[a] M. Luísa Serralheiro,[a] M. Eduarda Araújo,[a] Teresa Pamplona,[a] Susana Santos,[a]* M. Soledade Santos,[a] and Fátima Frazão[a,b]

[a]Departamento de Química e Bioquímica, CQB, Faculdade de Ciências da Universidade de Lisboa, 1749-016 Lisboa, Portugal
[b]Departamento de Ciências da Saúde, Universidade Lusófona, 1749-024 Lisboa, Portugal
*E-mail: smsantos@fc.ul.pt
Received July 7, 2010
DOI 10.1002/jhet.752
Published online 2 August 2011 in Wiley Online Library (wileyonlinelibrary.com).

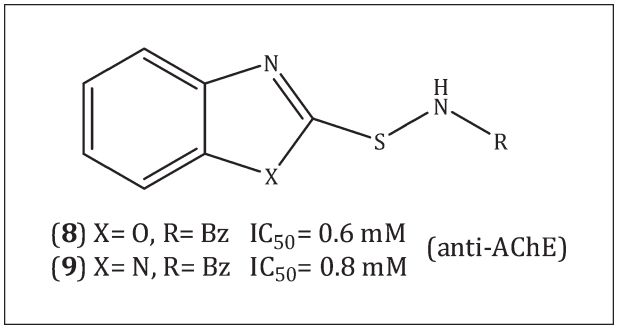

Several sulfenamide derivatives were designed as possible acetylcholinesterase (AChE) inhibitors. New sulfenamides were synthesized and proved to be stable under the physiological conditions used in the enzymatic assays. *N*-benzyl-2-benzoxazolylsulfenamide (8) and *N*-benzyl-2-benzimidazolylsulfenamide (9) revealed anti-AChE activity with IC_{50} values of 0.6 and 0.8 μ*M*, respectively, values of the same magnitude as those reported for galantamine and tacrine. The affinity for the biological site was evaluated in terms of interaction/partition toward sodium dodecyl sulfate (SDS) micelles. The inhibitory activity profiles were reasoned in terms of both partition toward a hydrophobic anionic environment and molecular geometry. The X—CSN dihedral angle deviations from collinearity stood out as a major parameter linked to enzyme specificity.

J. Heterocyclic Chem., **48**, 1287 (2011).

INTRODUCTION

Alzheimer's disease (AD) is a severe neurodegenerative disease characterized by an insidious onset with a chronic progressive course over months to years, which leads to a global cognitive decline. AD is one of the most serious health problems in the western world and accounts for the vast majority of age-related dementia, although it is no longer considered a natural consequence of aging. Pathologically, the disease is characterized by the presence of extracellular plaques of β amyloid (Aβ) peptides, and intracellular tangles of hyperphosphorylated tau protein, with the loss of neuronal synapses and pyramidal neurons [1]. Hence, agents that lower Aβ levels in the brain are considered potential therapeutic agents. However, despite the increasing number of anti-amyloid therapies under clinical development [2], at present, there is no way to reverse the damage or inhibit the formation of plaques and tangles, only cognitive enhancers may delay the cognitive decline. Drugs blocking natural hydrolysis metabolism of the neurotransmitter acetylcholine (ACh) allow a concentration increase of ACh over longer time periods in the synapses, stimulating cholinergic receptors [3]. Natural or synthetic drugs usually accomplish this blockage, by targeting the serine hydrolase acetylcholinesterase (AChE), an enzyme that hydrolyses ACh in higher eukaryotes. Some authors also postulate the role of this enzyme in the acceleration of the Aβ aggregation into amyloid plaques [4]. The identification of the three-dimensional structure of *Torpedo californica* acetylcholinesterase (TcAChE) was accomplished in 1991 [5] and since then it has been universally used as a model for the three dimensional structure of the enzyme. These studies revealed that the catalytic site is located in a deep and narrow gorge and comprises an esteratic site, an oxyanion hole, an anionic substrate binding site (AS), and an acyl binding site (ABS). Besides this catalytic site, a peripheral anionic site (PAS) plays a role in the conformation of the residues that fit inside the aromatic gorge and active site [6]. How these highly organized structures contribute to the catalytic efficiency of the enzyme is still an on-going discussion [7].

AChE inhibitors can be divided into those that bind noncovalently and reversibly, and those that form a covalent bond, which may act as slow substrates or inhibit the enzyme irreversibly, either by phosphorylating or carbamoylating the active site. The noncovalent inhibitors may vary in their structures and binding site of the enzyme, allowing many different starting points for drug design [8]. The search for AChE inhibitors clearly appears as a research niche worth focusing on, since only a few compounds presenting this ability (e.g., galantamine, tacrine, donepezil, and rivastigmine) are approved as commercial drugs.

In our on-going studies to find AChE inhibitors, we decided to synthesize several sulfenamides containing the heterocyclic moieties benzimidazole, benzoxazole, and benzothiazole and evaluate their *in vitro* activity against AChE. A common feature in the structure of most commercial drugs for AD is the presence of an aromatic ring and an amine function. It is now consensual that tacrine and its analogs exert its inhibitory action on AChE interacting with both the anionic subsite of the active site at the bottom of the gorge, and with the PAS, near its top, via aromatic stacking interactions with conserved aromatic residues [8]. It is likely that aromatic heterocyclic moieties of the compounds under study may interact the same way with AChE. Besides, more recently, benzothiazole and benzoxazole amine derivatives have been claimed to be AChE inhibitors [9]. Furthermore, because of the polarization of SN bond, sulfenamides are likely to react with nucleophiles on the sulfur atom [10] and so, the hydroxyl group of AChE serine residue may interact with the sulfenamide function of the compounds under study, rendering them potential enzyme inhibitors.

The anti AChE capacity of the sulfenamides was evaluated in terms of IC_{50}. The cell permeating ability was compared in terms of the lipophilic character, evaluated using sodium dodecyl sulfate micelles [11–16], and substituent induced changes of X—CSN and N=CSN dihedral angles, estimated with Molecular Modeling ProPlus.

RESULTS

Chemistry. Sulfenamides can be obtained by standard procedures, the condensation of an aryl or alkyl sulfenyl chloride with an amine being the most used general synthetic route. However, besides being poorly accessible, sulfenyl chlorides are very unstable and easily hydrolyzed [17], with side reactions usually occurring, leading to by-products, which render difficult the purification of the synthesized sulfenamides. The synthesis of sulfenamides can also be accomplished using more narrow scoped methods, such as oxidative condensation of thiols with amines [18], or metal-assisted reactions between disulfides and amines [19]. In the present work, we found that amides of sulfenic acid linked to a heteroatomic ring are best prepared by oxidative condensation of the corresponding thiol with an amine, using sodium hypochlorite (for *N*-unsubstituted sulfenamides) or iodine (for *N*-substituted sulfenamides) as the oxidizing agent [20]. These one-pot methods were slightly improved by keeping the pH of the solution between 12.2 and 12.5 throughout the reaction, even for *N*-substituted sulfenamides, which minimized side formation of the corresponding disulfide. Three classes of heteroaromatic sulfenamides were prepared with benzothiazole (X = S), benzoxazole (X = O), or benzimidazole (X = N) residues (Table 1). To evaluate the impact of the heteroatom in the activity, two homologous series were prepared for benzothiazole (**1–5**) and benzoxazole (**6–8**) derivatives. The extreme reactivity of benzimidazole derivatives made it impossible to obtain an equivalent series, being *N*-benzyl-2-benzimidazolylsulfenamide (**9**) the only compound to be successfully prepared. The chemical structure of the sulfenamides (Table 1) was elucidated by extensive spectroscopic studies (^1H and ^{13}C NMR, COSY, DEPT, HMQC, HMBC, and MS). To the best of our knowledge, compounds **3** and **6–9** were obtained for the first time. Compounds **1**, **2**, **4**, and **5**, though already reported in the literature, were spectroscopically characterized for the first time.

Table 1
Synthesized sulfenamides.

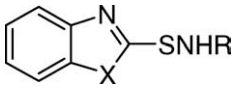

Compounds	X	R
1	S	H
2	S	CH_3CH_2
3	S	CH_2=$CHCH_2$
4	S	Bz
5	S	Ac
6	O	H
7	O	CH_3CH_2
8	O	Bz
9	N	Bz

***In* vitro AChE inhibitory activity.** All compounds synthesized were dissolved in methanol and proved to be stable (1 h, 25°C) in the Tris buffer used for the AChE activity assays. The stability tests were carried out by taking aliquots over 1 h, and analyzing the results by HPLC under the conditions described in the ''Experimental'' section. The inhibitory activity toward AChE (IC_{50} values in Table 2) for the synthesized compounds **1–9**, as well as for commercially available galantamine, used as reference standard, was evaluated according to Elman's method described in the ''Experimental''

Table 2

IC_{50} for Ache inhibition assays, partition coefficients toward SDS micelles, calculated Log *P* and Drug scores, and polar surface area, X—CSN and N=CSN dihedral angles for all sulfenamides.

Compounds	IC_{50}[a] (μ*M*)	$K_p \times 10^{-4}$	Log P[b]	Drug score[c]	Polar surface area (Å^2)[d]	Φ_{X-CSN} (°)	$\Phi_{N=CSN}$ (°)
1	2.1 ± 0.2	0.14	2.39	0.21	38.91	178	161
2	0.9 ± 0.1	2.63	2.84	0.25	24.92	180	−4
3	9.4 ± 1.6	1.15	2.87	0.18	24.92	−162	22
4	1.8 ± 0.1	0.36	3.67	0.22	24.92	−22	156
5	0.9 ± 0.1	3.84	2.44	0.26	45.15	105	−78
6	1.6 ± 0.2	1.3	1.68	0.52	52.05	175	−3
7	1.5 ± 0.1	>2.6	2.21	0.62	38.06	120	−60
8	0.6 ± 0.1	1.49	3.27	0.58	38.06	12	193
9	0.8 ± 0.1	2.11	2.71	0.68	40.71	10	192
Galantamine	0.7 ± 0.1	—	2.17	0.89	41.93	—	

[a] Results are expressed as mean (±SEM), $n = 3$.
[b] Estimated by AlOGPS 2.1 algorithm [34].
[c] Estimated by Osiris Property Explorer [35].

section. The results suggest that sulfenamides are promising AChE inhibitors with IC_{50} values between 0.60 and 9.4 μ*M*.

Comparing IC_{50} values for the benzothiazole derivatives **1** (R = H), **2** (R = CH_2CH_3), and **5** (R = Ac), an increase of about two times in the inhibitory activity was observed for the *N*-exocyclic substituted compounds, but the same tendency was not observed for the benzoxazole derivatives.

Concerning the electronegativity of the ring heteroatom, the IC_{50} results for *N*-benzyl derivatives **4**, **8**, and **9** showed, for both the benzoxazole (**8**) and benzimidazole (**9**) derivatives, containing the more electronegative heteroatoms, that is, oxygen and nitrogen, an increase in the inhibition capacity of about three times when compared to that of benzothiazole derivative (**4**).

The IC_{50} values presented in Table 2 for the *N*-substituted sulfenamides, particularly those for compounds **2**, **5**, **8**, and **9**, were of the same magnitude as the value obtained for galantamine in our laboratory (0.7 μ*M*). These values fell within the reported electric eel AChE IC_{50} inhibition data for galantamine (0.55 μ*M* [21]; 3.18 μ*M* [22]), and tacrine (0.044 μ*M* [23]; 0.18 μ*M* [24]). The AChE inhibition assays, monitored by HPLC, showed that sulfenamides were stable throughout the experiment, suggesting that they are responsible for the inhibition, and ruled out the possibility of any inhibitory activity due to their hydrolysis products. The Ser residue at the catalyst site does not seem to be able to catalyze the hydrolysis of the labile sulfenamide bond.

Membrane mimetic system permeability assays. The interaction of amphipathic and hydrophobic molecules with biomembranes is determinant for several cellular events, and the interaction of a solute with a microheterogeneous system may be quantitatively evaluated by its partition coefficient toward model membrane systems. The octanol/water biphasic system has been used to mimic the lipid–water interface, but this simplification has been criticized by several authors, who suggest that micelles, or synthetic phospholipidic bilayers are better biomembrane model systems. Reproducible results with phospholipidic bilayers are difficult and involve highly standardized experimental conditions to ensure homogeneous liposome composition and size distribution [14,25–28]. Micelles are well characterized and reproducible systems with minor spectral interferences, which may outshine minor differences between the compounds. These systems enable a preliminary screen of compound permeation capability and provide a lipophilicity profile outline, within a family of structurally related compounds. Low spectral resolution and high background signals characteristic of microheterogeneous systems have often been overcome, resorting to the application of second derivative spectrophotometry [29–31]. This procedure was used in this study to quantify the interaction of the new sulfenamides with sodium dodecyl sulfate (SDS) micellar aggregates and to evaluate the partition coefficients, K_p, compiled in Table 2. Partition coefficients toward sodium dodecyl sulfate micelles [14,27,32,33] were determined under the same experimental conditions as for the enzymatic assays (solvent mixture and buffer). To ensure the reliability of the K_p values obtained, Sparc online calculator v4.2, was used to evaluate p*K*a for all compounds, showing that they are all unionized at pH = 8. *N*-unsubstituted sulfenamides showed feebler signals and spectral shifts than the corresponding substituted derivatives, suggesting a stronger interaction of the latter with the membrane mimetic system. All sulfenamides studied present

relatively high K_p values, $\cong 10^4$ (Table 2), indicating a high affinity toward hydrophobic media with anionic character, and suggesting a general good membrane permeation capability [14,16,27,28]. *N*-substituted benzothiazolyl sulfenamides **2**–**5** showed higher partition coefficients than the unsubstituted one (**1**), with values ranging from 0.4×10^4 to 3.8×10^4, indicating that the substitution patterns studied facilitate partition. Comparing partition coefficients for the three benzyl derivatives (**4**,**8**,**9**) the benzimidazolylsulfenamide **9** showed the highest value (2.11×10^4) and the benzothiazolylsulfenamide **4** the lowest (0.36×10^4). The highest partition coefficient, among all compounds, was obtained for *N*-acetyl-2-benzothiazolylsulfenamide (**5**) (3.84×10^4).

Molecular modeling studies. Molecular properties that condition oral bioavailability are often considered in the development of bioactive molecules. In this study, a substrate focused screen for specific substrate–enzyme interactions, supported on geometric molecular properties, was undertaken.

Known algorithms [34,35] were used to estimate relevant parameters associated with drug oral bioavailability, namely log *P* (logarithm of octanol–water partition coefficient), log *S* (logarithm of aqueous solubility), overall drug score, polar surface area, and several molecular parameters, for example, molecular distances, angles, dihedral angles, and dipolar moments. This substrate molecule centered approach was used in an attempt to recognize which substrate geometric patterns could be linked to the targeting sites responsible for the observed biological activity. The geometric evaluation of the molecular parameters was performed with Molecular Modeling ProPlus, in an attempt to disclose potential stereochemical constraints associated with specific substitution patterns.

All compounds obeyed Verber *et al.* bioavailability model criteria [36], with few rotatable bonds (≤ 3) and small polar surface areas (25–52 Å^2). Estimated log *P* span from 1.68 to 3.67 while Osiris drug scores extend from 0.18 to 0.68; however, none of these parameters could explain by itself the experimentally observed inhibition profile. Furthermore, it is interesting to note that, excluding the nonsubstituted compounds **1** and **6**, there is a reasonable negative sign correlation between experimental log K_p and estimated log *P* (Fig. 1), which is indicative of micellar anionic headgroups–sulfenamides-specific interactions. Accordingly, the effect of specific interactions on molecular accessibility toward a hydrophobic environment with anionic character should be reasonably predicted by the partition toward SDS micelles.

However, compound's partition coefficients toward anionic micelles cannot account by themselves for the experimentally observed activity profile, thus pinpointing to other balancing effects possibly associated with

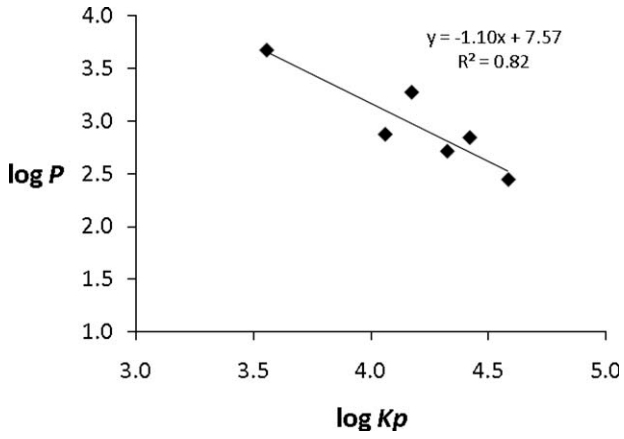

Figure 1. Correlation between calculated log *P* and experimentally determined log K_p.

stereochemical binding constraints at the enzyme active site. In view of the hydrophobic planar structure of the sulfenamide heteroaromatic ring, stereochemical constraints associated with binding of the sulfenamide function within the gorge are likely to be associated with dihedral angles Φ_{X-CSN} or $\Phi_{N=CSN}$, which were calculated and included in Table 2.

Overall, Φ_{X-CSN} dihedral angles span from $-162°$ to $180°$, whereas $\Phi_{N=CSN}$ span over a slightly narrower range ($-60°$ to $193°$), confirming the flatness of the heteroaromatic ring structure and suggesting that both ring heteroatoms are available for binding to the active site in opposing, but almost collinear positions. The values for the Φ_{X-CSN} dihedral angles support the expected flatness of the *N*-unsubstituted sulfenamides **1** and **6**, with values about 180° [Φ_{S-CSN} (**1**) = 178°; Φ_{O-CSN} (**6**) = 175°], and *N*-benzyl derivatives **4**, **8**, and **9**, with values close to 0° [Φ_{S-CSN} (**4**) = −22°; Φ_{O-CSN} (**8**) = 12°; Φ_{N-CSN} (**9**) = 10°]. In fact, benzyl substitution induces small rotations of the sulfenamide nitrogen atom, not compromising the almost coplanar structure of both rings, whereas alkyl substituents lead to larger rotations. These results also show a heteroatom size effect on *N*-unsubstituted sulfenamides, indicating that smaller Φ_{X-CSN} dihedral angles are observed for structures with smaller ring heteroatoms and suggesting that almost collinear N–X positions favor interaction/binding with AChE active site.

DISCUSSION

It is well known that the PAS of TcAChE [5], composed by several aromatic residues (Trp279, Tyr70, Tyr121, Asp72, Glu199, and Phe290) may bind bulky inhibitors. This includes compounds that do not penetrate into the gorge and bifunctional inhibitors, which are long enough to extend over it [37]. Furthermore, the

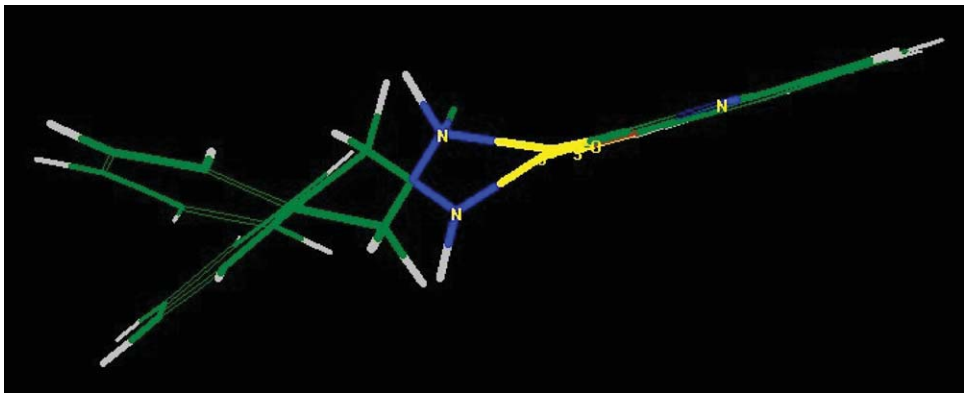

Figure 2. Most stable conformers of molecules **4** and **8** superimposed. [Color figure can be viewed in the online issue, which is available at wileyonlinelibrary.com.]

AS composed of Trp84, Glu199, and Phe330 may interact with inhibitors with secondary amines groups, through hydrogen-bonded water molecules [8] and with inhibitors with aromatic moieties, through π–π interactions favored by the hydrophobic environment of the aromatic rings from Trp and Phe. The most efficient AChE inhibitors interact with both the AS, at the bottom of the gorge, and with the PAS site, near its top. The synthesized compounds conjugate both the aromatic moiety and the amine function, apart from being relatively small molecules, which may diffuse rapidly and reach the anionic subsite. Among the compounds studied, the *N*-benzyl-2-benzoxazolylsulfenamide (**8**) and *N*-benzyl-2-benzimidazolylsulfenamide (**9**) stood out as the best inhibitors of AChE. Both these very hydrophobic compounds [K_p(**8**) = 1.5 × 10^4 and K_p(**9**) = 2.1 × 10^4] have two aromatic moieties and relatively coplanar structures with small X—CSN dihedral angle ($\Phi_{X-CSN} \cong 11°$), enabling the aforementioned π–π interactions. The difference in inhibitory activity between **8** and **9** may be related with the increased polar surface area of **9**. For benzothiazolylsulfenamide **4** the presence of a sulfur atom in the heteroaromatic ring results in a significant rotation of the benzyl substituent ($\Phi_{S-CSN} \cong -22°$). Figure 2 clearly demonstrates the rotation associated with the presence of oxygen or a sulfur atom in the heteroaromatic ring. This rotation coupled with the decrease in K_p, may account for the accentuated decrease observed in the inhibitory activity of **4**. Unsubstituted compounds **1** and **6** have larger polar surface areas than their benzyl derivatives and the most stable conformers also present a nearly coplanar arrangement, with the amine and the ring heteroatom in opposing directions [X—CSN dihedral angles ($\Phi_{X-CSN} \cong 177°$)], thus becoming less efficient inhibitors [IC_{50}(**1**) > IC_{50}(**4**) and IC_{50}(**6**) > IC_{50}(**8**)]. The increased inhibitory activity of compound **6** over the corresponding **1** may be linked to the larger K_p [K_p(**6**) > K_p(**1**)]. Compound **5**, despite its polarity, showed the highest partition coefficient toward SDS micelles [K_p (**5**) ≅ 3.8 × 10^4], an affinity that may partially overcome an inadequate geometry, characterized by a noncoplanar dihedral angle ($\Phi_{S-CSN} \cong 105°$), thus justifying why this is not the most efficient AChE inhibitor. The increased activity of *N*-ethyl-2-benzothiazolylsulfenamide (**2**) over compound **1**, may also be enlightened considering minor differences between their X—CSN dihedral angles ($\Phi_{S-CSN} \cong 180°$) coupled with a more favorable partition coefficient [K_p (**2**) ≅ 2.6 × 10^4 > K_p (**1**)], and a reduction in the polar surface area. The competition between partition coefficients and an extremely adverse binding geometry ($\Phi_{S-CSN} \cong 120°$) may account for the significant increase of IC_{50} for benzoxazolylsulfenamide **7** relatively to compound 2. Data for compound **3** reinforces the relevance of the S—CSN dihedral angle ($\Phi_{S-CSN} \cong -162°$) indicating, once again, that a significant partition coefficient ($K_p \cong 1.15 \times 10^4$) cannot outrun a very poor geometry, which seems to dictate the low inhibitory activity of this compound**.** Additionally, the inhibitory activity of ethyl derivatives is larger for the benzothiazolyl series, a feature which may also be rationalized considering the increased rotation of the dihedral angle associated with ring heteroatom substitution of sulfur by oxygen, which involves a rotation toward an inadequate geometry**.**

CONCLUSIONS

The heteroaromatic sulfenamides described, herein, were designed, synthesized, and tested for their anti AChE activity. The compounds revealed good inhibition with IC_{50} values between 0.6 and 9.4 μ*M* with *N*-benzyl-2-benzoxazolylsulfenamide (**8**) and *N*-benzyl-2-benzymidazolylsulfenamide (**9**) showing the best AChE inhibition capacity, comparable with literature values for galantamine and tacrine. These compounds are uncharged at

pH = 8, their geometry, partition coefficients, and polar surface areas suggest that they may permeate membranes to exert their action inside the cells, rendering them promising lead structures in the search for new AChE inhibitors.

The inhibitory activity profiles found for all the sulfenamides synthesized can be reasoned in terms of a balance between partition toward a hydrophobic anionic environment, polar surface area, and deviations of X—CSN dihedral angles from colinearity, which emerges as a factor potentially coupled to enzyme specificity. Furthermore, the integrity of the sulfenamide molecules, throughout enzyme inhibition assays, implies a noncovalent interaction with the enzyme.

In summary, these results suggest that compounds **8** and **9** could be considered as new leads for further optimization.

EXPERIMENTAL

Melting points were measured in a Stuart Scientific-melting point apparatus SMP3. IR spectra were obtained using a Hitachi 270–50 spectrophotometer on KBr pastille and only diagnostic bands are reported on a cm^{-1} scale. ^1H NMR and ^{13}C NMR spectra were acquired in a Brucker Avance 400 apparatus at 400 and 100.4 MHz, respectively, using chloroform-*d* or d_6 DMSO as solvents. The chemical shifts are reported in parts per million (ppm, δ), using the appropriate signal for residual solvent protons as reference. Coupling constants are reported to the nearest 0.1 Hz. HRMS were recorded on a Finnigan FT/MS 2001-DT mass spectrometer. Column chromatography used silica-gel 60, 0.040–0.063 μm (*Merck* 9385). Thin layer chromatography (TLC) and preparative TLC were performed on precoated silica-gel 60 F254 (*Merck* 5554 and *Merck* 5717, respectively).

HPLC studies were carried out in isocratic mode (methanol/water 8:2, 1 mL min^{-1}) using a Surveyor Plus HPLC system (Thermo Finnigan) equipped with a Surveyor Autosampler Plus with a 100 μL loop, a quaternary pump Surveyor LC Pump Plus, and a diode-array detector Surveyor PDA Plus. A stainless-steel Thermo Electron Hypersil GOLD C18 column (100 × 4.6 mm^2, particle size 5 μm) or a Merck Purospher® Star RP-18 endcapped column (125 × 4 mm^2, particle size 5 μm) were used.

CMCs were determined in thermostatic vessels at 25.0 ± 0.1°C with a Krüss K100M2 tensiometer coupled to a Metrohm 765 Dosimat automatic burette.

UV–vis scans were performed at 25°C with Shimadzu UV 1603–visible spectrophotometer coupled to a Shimadzu CPS 240A peltier module.

All purchased starting materials and reagents were used without further purification unless stated otherwise. All chemicals were of analytical grade. AChE type VI-S, from electric eel 349 U mg^{-1} solid, 411 U mg^{-1} protein, 5,5′-dithiobis[2-nitrobenzoic acid] (DTNB), acetylthiocholine iodide (AChI), tris[hydroxymethyl]aminomethane (tris buffer) and sodium dodecyl sulfate were obtained from Sigma.

General procedure for the synthesis of compounds 1–9. Synthesis of 2-benzoxazolylsulfenamide (**6**) is described as an example of the procedure followed for preparation of *N*-unsubstituted sulfenamides:

Benzoxazole-2-thiol (1 g, 10 mmol) was dissolved in 5 mL of NaOH 2*M*. This solution and 22.5 mL of 13% sodium hypochlorite were dropped slowly at equal rates into 18 mL of concentrated ammonium hydroxide (25%v/v). The mixture was stirred during addition and cooled in ice-bath (5–10°C) until stabilization of pH between 12.2 and 12.0. The precipitate obtained was washed with cold water until free from alkali and crystallized from pentane; yield 49%.

Synthesis of *N*-ethyl-2-benzoxazolylsulfenamide (**7**) is described as an example of the procedure followed for preparation of *N*-substituted sulfenamides:

Benzoxazole-2-thiol (2.5 g, 1.65 mmol) was dissolved in 68.8 mL of NaOH 0.48*M*. To this solution, 26.5 mL of a 70% aqueous solution of ethylamine and iodine (8.39 g, 0.033 mol) dissolved in 55 mL of a 0.5*M* aqueous solution of potassium iodide were added dropwise. The pH was kept between 12.2 and 12.0 until precipitation of the sulfenamide, which was washed with cold water and crystallized from petroleum ether; yield 80.9%.

2-Benzothiazolylsulfenamide (1). Yellow crystals η 87%. Mp 124–126°C dec. (lit. [20] 127–128°C). IR (KBr); ν_{max}/cm^{-1}: 3323, 3198, 1461, 1429, 1313, 1242, 1031, 692. RMN ^1H (400 MHz; $CDCl_3$) δ 7.82 (2H, m, H-5, H-6); 7.43 (1H, m, H-4); 7.31 (1H, m, H-7); 3.32 (2H, s, NH_2); NMR ^{13}C (100 MHz; $CDCl_3$) δ 178.3 (C-2, C); 154.6 (C-9, C); 135.0 (C-8, C); 126.0 (CH, C-4); 123.8 (CH, C-7); 121.6 (CH, C-5); 121.2 (CH, C-6).

N-Ethyl-2-benzothiazolylsulfenamide (2). Yellow crystals η 62%. Mp 54.5–55.7°C (lit. [20] 55–57°C). IR (KBr); ν_{max}/cm^{-1}: 3225, 2920, 2880, 1458, 1427, 1238, 1022, 752. RMN ^1H (400 MHz; $CDCl_3$) δ 7.84 (1H, d, J = 8.4 Hz, H-4); 7.82 (1H, d, J = 7.6 Hz, H-7); 7.42 (1H, ddd, J = 8.4; 7.6; 1.2 Hz, H-5); 7.29 (1H, ddd J = 7.6; 1.2 Hz, H-6); 3.32 (1H, s_b, NH); 3.22 (2H, dq, J = 7.2; 5.6 Hz, H-1′); 1.27 (3H, t, J = 7.2 Hz, H-2′). NMR ^{13}C (100 MHz; $CDCl_3$) δ 178.6 (C-2, C); 154.9 (C-9, C); 135.0 (C-8, C); 125.9 (CH, C-4); 123.7 (CH, C-7); 121.6* (CH, C-5); 121.1* (CH, C-6); 47.5 (CH_2, C-1′); 15.7 (CH_3, C-2′).

N-Ethenyl-2-benzothiazolylsulfenamide (3). Pale yellow crystals η 34.1%. Mp 38.5–40.0°C. IR (KBr); ν_{max}/cm^{-1}: 3191, 3079, 3001, 2881, 1454, 1428, 1311, 1241, 1007, 754, 725. NMR ^1H (400 MHz; $CDCl_3$) δ 7.84 (1H, d, J = 8.4 Hz, H-4); 7.82 (1H, d, J = 7.6 Hz, H-7); 7.42 (1H, ddd J = 8.4; 7.8; 1.2 Hz, H-5); 7.30 (1H, ddd J = 7.4; 1.2 Hz, H-6); 5.99 (1H, ddd, J = 17.2; 10.2; 1.2 Hz, H-2′); δ 5.30 (1H, dd, J = 17.0; 1.2 Hz, H-3′a); 5.24 (1H, dd, J = 10.2; 1.2 Hz, H-3′b); 3.37 (2H, t, J = 6.0 Hz, H-1′); 3.43 (1H, t_b, NH). HRMS $[M]^+$ m/z 222.02790 (calcd. for $C_{10}H_{10}N_2S_2$ 222.02799).

N-Benzyl-2-benzothiazolylsulfenamide (4). Yellow crystals η 42%. Mp 115.0–116.5°C dec. (lit. [20] 117°C). IR (KBr); ν_{max}/cm^{-1}: 3081, 3025, 1467, 1429, 1311, 1238, 1079, 1005, 696. NMR ^1H (400 MHz; $CDCl_3$) δ 7.87 (2H, m, H-4, H-7); 7.44 (5H, m, H-2′, H-3′, H-4′, H-5′, H-6′); 7.34 (2H, m, H-6, H-5); 4.37 (2H, d, J = 8 Hz, CH_2N); 3.67 (1H, s, NH). NMR ^{13}C (100 MHz; $CDCl_3$) δ 177.4 (C-2, C); 154.9 (C-9, C); 138.5 (C-1′, C); 135.2 (C-8, C); 128.7 (C-2′, CH); 128.5 (C-3′, CH); 128.0 (C-4′, CH); 126.0 (C-4, CH); 123.8 (C-7, CH); 121.7 (C-5, CH); 121.2 (C-6, CH); 57.1 (CH_2N).

N-Acetyl-2-benzothiazolylsulfenamide (5). White crystals η 31.5%. Mp 133.8–135.8°C (lit. [20] 135–136°C). IR (KBr); ν_{max}/cm^{-1}: 3394, 3177, 3064, 2877, 2733, 1685, 1482–1426, 1308, 1255). NMR ^1H (400 MHz; $CDCl_3$) δ 10.35 (1H, s, H-11); 8.02 (1H, d; J = 8 Hz, H-4); 7.84 (1H, d; J = 8 Hz, H-7); 7.47 (1H, t, J = 8 Hz, H-5); 7.36 (1H, t, J = 8 Hz,

H-6)); 2.16 (3H, s, CH_3). NMR ^{13}C (100 MHz; $CDCl_3$) δ 173.2 (C=O, C-1′); 171.4 (C, C-2); 153.8 (C, C-9); 134.1 (C, C-8); 126.4 (CH, C-4); 124.3 (CH, C-7); 121.8* (CH, C-5); 121.4* (CH, C-6); 22.7 (CH_3, C-2′).

2-Benzoxazolysulfenamide (6). Pink amorphous powder η 49.1%. IR (KBr); ν_{max}/cm^{-1}: 3352, 3228, 1508, 1452, 1236, 1094, 750, 735, 690. NMR ^1H (400 MHz; $CDCl_3$) δ 7.64 (1H, d, J = 7.5 Hz, H-7); 7.48 (H, d, J = 7.5 Hz, H-4); 7.33 (1H, ddd, J = 1.2; 7.5; 7.5 Hz, H-6*); 7.27 (1H, ddd, J = 1.3; 7.5; 7.5 Hz, H-5*); 3.23 (2H, s, NH_2) NMR ^{13}C (100 MHz; $CDCl_3$) δ 169.7 (C-2, C); 152.2 (C-9, C); 141.7 (C-8, C); 124.5 (C-6, CH); 124.0 (C-5, CH); 118.5 (C-4, CH); 110.2 (C-7, CH). HRMS $[M]^+$ *m/z* 166.02058 (calcd. for $C_7H_6N_2OS$ 166.02008).

N-Ethyl-2-benzoxazolylsulfenamide (7). Yellow oil 80.9%. IR (KBr); ν_{max}/cm^{-1}: 3246, 2971, 2932, 1499, 1452, 1236, 1127, 1093, 742. NMR ^1H (400 MHz; $CDCl_3$) δ 7.64 (1H, d, J = 7.8 Hz, H-4); 7.5 (1H, d, J = 8.0 Hz, H-7); 7.29 (2H, m, H-5, H-6); 3.48 (1H, t_b, NH); 3.22 (2H, dq, J = 7.2 Hz, H-1′); 1.23 (3H, t, J = 7.2 Hz, H-2′). NMR ^{13}C (100 MHz; $CDCl_3$) δ 168.0 (C-2, C); 151.8 (C-9, C); 141.9 (C-8, C); 124.3 (C-6, CH); 123.9 (C-5, CH); 118,6 (C-4, CH); 110.1 (C-7, CH); 40.9 (C-1′, CH_2); 15.0 (C-2′, CH_3). HRMS $[M]^+$ *m*/z 194.05158 (calcd. for $C_9H_{10}N_2OS$ 194.05083).

N-Benzyl-2-benzoxazolylsulfenamide (8). Pink whitish crystals η 53%. Mp 54.1–55.0°C. IR (KBr); ν_{max}/cm^{-1}: 3355, 3062, 3027, 2988, 2822, 1495–1422, 1231, 1209, 698. NMR ^1H, (400 MHz;$CDCl_3$) δ 7.70 (1H, d, J = 8 Hz, H-4); 7.50 (1H, J = 8 Hz, H-7); 7.44 (5H, m, H-2′, H-3′, H-4′, H-5′, H-6′); 7.34 (1H, m, H-6); 7.30 (1H, m, H-5); 4.37 (2H, d, J = 8 Hz, CH_2N); 3.67 (1H, s, NH) NMR ^{13}C (100 MHz; $CDCl_3$) δ 167.6 (C-2, C); 152.0 (C-9, C); 141.9 (C-8, C); 138.2 (C-1′, C); 128.6 (C3′, C-5′, CH); 128.6 (C-2′, C-6′, CH); 127.9 (C-4′, CH); 124.4 (C-6, CH); 124.0 (C-5, CH); 118.8 (C-4, CH); 110.2 (C-7, CH); 56.5 (CH_2N). HRMS $[M]^+$ *m*/z 256.06671 (calcd. for $C_{14}H_{12}N_2OS$ 256.06648).

N-Benzyl-2-benzimidazolylsulfenamide (9). White crystals η 10.82%. Mp 117.0–117.5°C dec. IR (KBr); ν_{max}/cm^{-1}: 3309, 3052, 3031, 2956, 2808, 1494, 1400, 1283, 1245, 696. NMR ^1H (400 MHz; $CDCl_3$) δ 7.52 (2H, m, H-4, H-7); 7.52 (5H, m, H-2′, H-3′, H-4′, H-5′, H-6′); 7.22 (2H, m, H-7, H-8); δ 4.21 (2H, d, CH_2); 3.60 (1H, s, NH). NMR ^{13}C (100 MHz; $CDCl_3$) δ 162.2 (C-2, C); 154.3 (C-9, C-8, C); 138.6 (C-1′, C); 128.8 (C3′, C-5′, CH); 128.5 (C-2′, C-6′, C-6, C-5, CH); 128.1 (C-4′, CH);); 122.2 (C-4,C-7,-CH); 57.3 (CH_2N). HRMS $[M+H]^+$ *m*/z 256.09398 (calcd. for $C_{14}H_{13}N_3S$ 256.09029).

Stability studies. The stability of sulfenamides, dissolved in methanol, was evaluated (1 h, 25°C) in the buffer used for the activity assays, and the studies were accomplished by HPLC, as described in above. For each assay, 100 μL of sample was withdrawn each 10 min during 1 h and dissolved to 1 mL in the methanol. Tris buffer (pH 8) was used for the stability studies.

AChE inhibitory activity. AChE enzymatic activity was measured using an adaptation of the method described by Ingkaninan *et al*. [38]. One hundred and eighteen microliters of 50 m*M* Tris-HCl buffer (pH = 8), 10 μL of MeOH compound solution, and 7.5 μL of AChE solution (0.26 U/mL) were mixed in a microwell plate and left to incubate for 15 min. Subsequently, 22.5 μL of a solution of AChI (0.023 mg/mL) and 142 μL of 3 m*M* DTNB were added. The reaction was carried out at 20°C**.** The absorbance was read at 405 nm when the reaction reached the equilibrium. A control reaction was carried out using water instead of the inhibitor, and it was considered 100% activity.

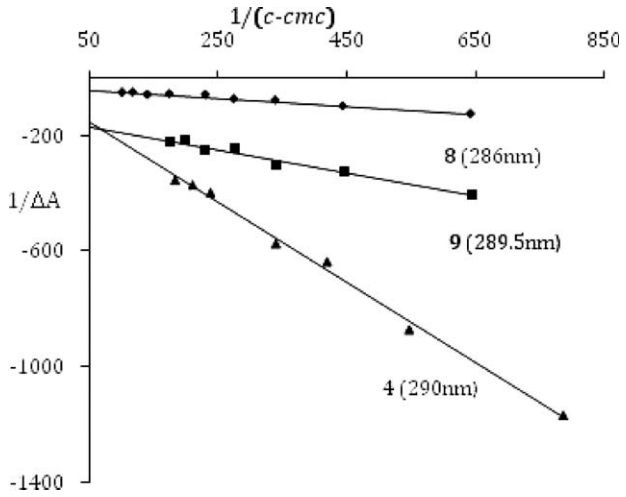

Figure 3. Evaluation of partition coefficients for sulfenamides **4**, **8**, and **9** toward sodium dodecyl sulfate micelles [eq. (2)].

$$I\ (\%) = 100 - (A_{sample}/A_{control}) \times 100 \qquad (1)$$

where A_{sample} is the absorbance of the enzyme reaction in the presence of sulfenamide and $A_{control}$ the absorbance of the control reaction. Tests were carried out in triplicate and a blank with Tris-HCl buffer instead of enzyme solution was used. For sulfenamides, a blank with methanol was carried out.

Membrane mimetic system permeability assays. Partition coefficients toward sodium dodecyl sulfate micelles were determined resorting to second derivative spectrophotometry studies [30,31] under the same conditions of the biological assays. The changes in the absorption spectrum of solutes associated with the presence of micellar aggregates allow the discrimination between molecules in the different solubilization environments enabling the quantification of free or micelle-bound solute, whenever solute micellar binding/incorporation is accompanied by appropriate spectral shifts [14,27]. Sodium dodecyl sulfate critical micelle concentration (CMC) in the presence of MeOH (3%), and Tris buffer was determined through surface tension measurements, using a titrimetric procedure, and resorting to Gibbs equation (CMC = $1.23 \times 10^{-3}M$) [32,36,39–41].

The partition toward a micellar pseudo phase is described by a saturation curve, therefore, if the CMC is known, K_p($K_p = x_{sulf,mic}/x_{sulf,w}$) where $x_{sulf,w}$ and $x_{sulf,mic}$ are equilibrium sulfenamide mole fractions in aqueous and micellar media) can be determined.

K_p can be obtained either by nonlinear iterative fit or from the linearized plots.

$$\frac{1}{\Delta A} = \frac{1}{\Delta\varepsilon l[\mathrm{Sulf}]_{w,0}} + \frac{1}{\Delta\varepsilon l[\mathrm{Sulf}]_{w,0}K_p}\frac{[W]}{(c - \mathrm{cmc})} \qquad (2)$$

where ΔA and $\Delta\varepsilon$ correspond to the variation in absorption and molar absorbtivity associated with the presence

of micellar aggregates, $[Sulf]_{w,0}$ is the initial sulfenamide molar concentration in the absence of surfactant, [W] is the molar concentration of water, and c is the surfactant molar concentration.

The slopes and intercepts of linearized plots ($r^2 > 0.98$), such as those presented in Figure 3 for compounds **4**, **8**, and **9**, were used to calculate K_p. The values, presented in Table 2, are weighed averages two to four independent experiments, for sulfenamide concentrations in the range of 0.1–0.5 μM, and pertain to determinations made at least at two wavelengths for each sulfenamide.

Molecular modeling studies. Molecular Modeling ProPlus chemistry software from Norgwyn Montgomery Software was used to drawn all compound. After a conformational analysis, the geometry was optimized, and finally the molecular dimensions, angles, and dihedral angles were obtained for the most stable conformer.

Acknowledgments. The authors thank Fundação para a Ciência e Tecnologia (POCTI/QUI/59328/2004) for financial support.

REFERENCES AND NOTES

[1] Pimplikar, S. W. Int J Biochem Cell Biol 2009, 41, 1261.

[2] Pangalos, M. N.; Jacobsen, S. J.; Reinhart, P. H. Biochem Soc Trans 2005, 33, 553.

[3] Heinrich, M.; Teoh, H. L. J Ethnopharmacol 2004, 92, 147.

[4] Ferrari, G. V.; Canales, M. A.; Shin, I.; Weiner, L. M.; Silman, I.; Inestrosa, N. C. Biochemistry 2001, 40, 10447.

[5] Sussman, J. L; Harel, M.; Frolow, F.; Oefner, C.; Goldman, A.; Toker, L.; Silman, I. Science 1991, 253, 872.

[6] Lin, G.; Lai, C. Y.; Liao, W. C. Bioorg Med Chem 1997, 2683.

[7] Paz, A.; Xie, Q.; Greenblatt, H. M.; Fu, W.; Tang, Y.; Silman, I.; Qiu, Z.; Sussman, J. L. J Med Chem 2009, 52, 2543.

[8] Greenblatt, H. M.; Dvir, H.; Silman, I.; Sussman, J. L. J Mol Neurosci 2003, 20, 369.

[9] Villalobos, A.; Arthur, N.; Chen, Y. L. US Patent 6,498,255,2002.

[10] Guarino, V. R.; Karunaratne, V.; Stella, V. J. Bioorg Med Chem Lett 2007, 17, 4910.

[11] Leo, A.; Hansch, C.; Elkins, D. Chem Rev 1971, 71, 525.

[12] Treiner, C.; Vaution, C.; Cave, G. N. J Pharm Pharmacol 1982, 34, 539.

[13] Treiner, C. J Colloid Interface Sci 1983, 93, 33.

[14] Sepulveda, L.; Lissi, E.; Quina, F. Adv Colloid Interface Sci 1986, 25, 1.

[15] Seydel, J. K.; Wiese, M. In Drug-Membrane Interactions: Analysis, Drug Distribution, Modeling; Mannhold, R.; Kubinyi, H.; Folkers, G., Eds.; Wiley-VCH, Weinheim, 2002, pp 35–50.

[16] Suomalainen, P.; Johans, C.; Soderlund, T.; Kinnunen, P. K. J. J Med Chem 2004, 47, 1783.

[17] Davis, F. A. J Org Chem 2006, 71, 8993.

[18] Bowman, W. R.; Marmon, R. J. In Comprehensive Organic Functional Group Transformations; Katritzky, A. R.; Meth-Cohn, O.; Rees, C. W., Eds,; Elsevier Science: Oxford, 1995, p 333.

[19] Illyés, T-Z.; Molnar-Gabor, D.; Szilágy, L. Carbohydr Res 2004, 339, 1561.

[20] Carr, E. L.; Smith, G. E. P., Jr.; Alliger, G. J Org Chem 1949, 14, 921.

[21] Tang, H.; Wei, Y.-B.; Zhang, C.; Ning, F.-X.; Qiao, W.; Huang, S.-L.; Ma, L.; Huang, Z.-S.; Gu, L.-Q. Eur J Med Chem 2009, 44, 2523.

[22] Lee, S.-S.; Venkatesham, U.; Rao, C. P.; Lam, S-H.; Lin, J-H. Bioorg Med Chem 2007, 15, 1034.

[23] Alptüzün, V.; Prinz, M.; Hörr, V.; Scheiber, J.; Radacki, K.; Fallarero, A.; Vuorela, P.; Engels, B.; Braunschweig, H.; Erciyas, E.; Holzgrabe, U. Bioorg Med Chem 2010, 18, 2049.

[24] Marco-Contelles, J.; León, R.; de los Ríos, C.; Guglietta, A.; Terencio, J.; López, M. G.; García, A. G.; Villarroya, M. J Med Chem 2006, 49, 7607.

[25] Gutierrez-Pichel, M.; Barbosa, S.; Taboada, P.; Mosquera, V. Colloid Polym Sci 2003, 281, 575.

[26] Fujita, T.; Hansch, C.; Iwasa, J. J Am Chem Soc 1964, 86, 5175.

[27] Liu, W. Y.; Guo, R. J Colloid Interface Sci 2006, 302, 625.

[28] Reis, S.; Moutinho, C. G.; Pereira, E.; de Castro, B.; Gameiro, P.; Lima J. J Pharm Biomed Anal 2007, 45, 62.

[29] Hosseinzadeh, R.; Gheshlagi, M.; Tahmasebi, R.; Hojjati, F. Cent Eur J Chem 2009, 7, 90.

[30] Kitamura, K.; Imayoshi, N.; Goto, T.; Shiro, V.; Mano, T.; Nakai, Y. Anal Chim Acta 1995, 304, 101.

[31] Pola, A.; Michalak, K.; Burliga, A.; Motohashi, N.; Kawase, M. Eur J Pharm Sci 2004, 21, 421.

[32] Fuguet, E.; Rafols, C.; Roses, M.; Bosch, E. Anal Chim Acta 2005, 548, 95.

[33] Tanaka, A.; Ikeda, S. Colloids Surf 1991, 56, 217.

[34] http://www.vclab.org/lab/alops (accessed February 2010).

[35] http://www.organic-chemistry.org/prog/peo (accessed February 2010).

[36] Veber, D.; Johnson, S.; Cheng, H-Y.; Smith, B.; Ward, K.; Kopple, K. J Med Chem 2002, 45, 2615.

[37] Harel, M.; Hyatt, J. L.; Brumshtein, B.; Morton, C. L.; Yoon, K. J. P.; Wadkins, R. M.; Silman, I.; Sussman, J. L.; Potter, P. M. Mol Pharmacol 2005, 67, 1874.

[38] Ingkaninan, K.; Temkitthawon, P.; Chuenchom, K. J Ethnopharmacol 2003, 89, 261.

[39] Fisicaro, E.; Compari, C.; Duce, E.; Biemmi, M.; Peroni, M.; Braibanti, A. Phys Chem Chem Phys 2008, 10, 3903.

[40] Rodriguez, A.; Graciani, M. D.; Moya, M. L. Langmuir 2008, 24, 12785.

[41] Chauhan, M. S.; Kumar, G.; Kumar, A.; Sharma, K.; Chauhan, S. Colloids Surf A Physicochem Eng Asp 2001, 180, 111.